Malaysian Journal of Analytical Sciences (MJAS)



Published by Malaysian Analytical Sciences Society

SYNTHESIS, CHARACTERIZATION AND ELECTROCHEMICAL STUDIES OF TRANSITION METAL COMPLEXES CONTAINING 3,6-BIS(3,5-DIMETHYLPYRAZOLYL) PYRIDAZINE LIGAND

(Sintesis, Pencirian dan Kajian Elektrokimia bagi Kompleks Logam Peralihan Mengandungi Ligan 3,6-Bis(3,5-Dimetilpirazolil) Piridazina)

Shankary Selvanathan and Woi Pei Meng*

Department of Chemistry, Faculty of Science, Universiti Malaya, 50603 Kuala Lumpur, Malaysia

*Corresponding author: pmwoi@um.edu.my

Received: 2 November 2020; Accepted: 21 January 2021; Published: xx February 2021

Abstract

Four novel coordination complexes were synthesized based on 3,6-bis (3,5-dimethylpyrazolyl) pyridazine ligand with Cu(II), Fe(II), Ni(II) and Co(II) metals. The synthesized complexes were characterized using several analyses. The infrared (IR) spectra for all the complexes showed a significant shift at the ligand methyl group (C-H), pyrazole ring (C=N), pyridazine ring (C-N) and (N-N) at 2926 cm⁻¹, 1137 cm⁻¹, 1162 cm⁻¹ and 970 cm⁻¹, respectively. The elemental analyses of the complexes confined to the stoichiometry of 1:2 ratio between the ligand and the metal cation. The presence of the metal in the complexes was confirmed using the FESEM-EDX analysis. The complexation of the metals to the ligand was evidenced when all the complexes exhibit a significant shift in the position of the characteristic ligand band at around 260 nm due to the HOMO \rightarrow LUMO $\pi \rightarrow \pi^*$ transitions of the pyridazine and pyrazoles groups in the UV-Vis spectrum. Cyclic voltammetry (CV) method was used to explore the redox characteristics of the complexes. The Cu(II), Fe(II) and Ni(II) complexes exhibited quasi-reversible single electron transfer process while no peak was observed in Co(II) complex upon scanning from -1.5 to 1.5 V vs. Ag/AgCl. This observation is speculated to be the effect of poor complexation in between the metal and the ligand. The potential recorded for Cu(II) complex at 0.03 V vs. Ag/AgCl was corresponded to the reduction of Cu(II) to Cu(I) while the potential at 0.75 V was due to the oxidation of Cu(I) to Cu(II). For the Fe(II) complex, the redox couple Fe(II)/Fe(III) was recorded at -0.47 V and -0.67 V during its oxidation and reduction process respectively. Finally, the peak at 0.71 V in the CV of Ni(II) complex is attributed to its oxidation process of Ni(I) to Ni(II) while the peak at 0.12 V is due to its reduction from Ni(II) to Ni(I).

Keywords: pyridazine, transition metal, coordination complex, electrochemical behavior

Abstrak

Empat kompleks koordinatan novel telah disintesis berdasarkan ligan 3,6-bis(3,5-dimetilpirazolil) piridazina dengan logam Cu(II), Fe(II), Ni(II) dan Co(II). Kompleks yang disintesis dicirikan dengan beberapa kaedah analisis. Spektrum IR bagi kesemua kompleks menunjukkan perubahan yang ketara pada kumpulan metil ligan (C-H), lingkaran pirazol (C=N), lingkaran piridazina (C-N) and (N-N) masing-masing pada 2926 cm⁻¹, 1137 cm⁻¹, 1162 cm⁻¹ and 970 cm⁻¹. Analisis unsur kompleks membataskan nisbah stoikiometri ligan: logam kepada 1: 2. Kehadiran logam dalam kompleks juga telah disahkan menerusi analisis FESEM-

EDX. Pembentukan kompleks bersama logam dan ligan disahkan lebih lanjut kerana semua kompleks mempamerkan perubahan yang sangat ketara dalam pencirian pada 260 nm kerana peralihan HOMO \rightarrow LUMO $\pi \rightarrow \pi^*$ dalam lingkaran pirazol and piridazina menerusi spektrum UV-Vis. Sifat redoks kompleks telah disiasat dengan kaedah elektrokimia voltammetri kitaran (CV). Kompleks Cu(II), Fe(II) dan Ni(II) mempamerkan proses pemindahan elektron tunggal yang seakan-balik manakala tiada puncak diperhatikan bagi kompleks Co(II) apabila kesemua kompleks ini diimbas pada potensi -1.5 ke 1.5 V vs. Ag/AgCl. Potensi untuk kompleks Cu(II) pada 0.03 V vs. Ag/AgCl sepadan dengan penurunan Cu(II) kepada Cu(I) manakala potensi pada 0.75 V adalah disebabkan oleh pengoksidaan Cu(I) kepada Cu(II). Bagi kompleks Fe(II), pasangan redoks Fe(II)/Fe(III) mencatatkan potensi masing-masing pada -0.47 V dan -0.67 V semasa proses pengoksidaan dan penurunan. Akhirnya, potensi pada 0.71 V dalam voltammogram kitaran kompleks Ni(II) adalah disebabkan oleh proses pengoksidaan Ni(II) kepada Ni(I) manakala potensi pada 0.12 V adalah disebabkan oleh penurunan dari Ni(II) ke Ni(I).

Kata kunci: piridazina, logam peralihan, kompleks koordinatan, tindakan elektrokimia

Introduction

Coordination chemistry is an interesting field of study which assimilates both the traditional inorganic and organic chemistry disciplines by segregating a new class of compounds, comprising a central metallic atom bound to a group of organic molecules, known as metal complexes [1]. These metal complexes possess valuable chemical properties, which pave the way to a variety of applications, particularly as catalysts in various chemical reactions. One of such prospective applications is in the field of electrocatalysis.

Amongst all the other types of metal atoms, transition metals are the commonly used metal center in electrocatalytic metal complexes, namely in catalyzing reaction with having strong interests in environmental conservation such as hydrogen evolution, carbon dioxide reduction and water oxidation processes [2]. The first-row transition metals have been the center of attraction of this research due to a few advantages possessed by them. One of which is their lower toxicity property compared to other row transition metals which makes it a suitable choice of metals in order to pursue a green chemistry method. In addition, the 3d transition metals can be found more abundantly in nature.

The electronic arrangement of transition metals allows them to exist in a variety of oxidation states and they are also able to interchange between the oxidation states, form complexes with the reagent and be a good source for electrons. These characteristics help transition metal complexes to catalyze many redox reactions in nature. The catalytic ability of the transition metal complexes is exploited when it is coupled to an electrochemical cell in which it catalyzes the redox reactions of specific substrate. A fascinating feature in this application is the capacity to alter the potential of the redox reaction by manipulating the metal centers and the corresponding ligands [3].

One of the widely used ligands in coordination chemistry are pyridazines. The two nitrogen atoms in the heterocyclic structure of pyridazine allow it to coordinate with two metal centers close to each other [4]. On the other hand, pyrazole is classified as a five membered aromatic structure comprising three carbons and two nitrogens. The idea of having both the sixmembered ring structure such as pyridazine and five-membered ring structure such as pyrazole combined as one ligand provides an interesting dimension and geometry upon binding with metals. In return, the complexes of such ligands are expected to have a different electronic properties [5].

The target ligand in this study, 3,6-bis-(3,5-dimethylpyrazolyl)-pyridazine is one of such unique ligand molecules that contain both pyridazine and pyrazolyl structures. The ability of the ligand to form a metallacycle leads to a stable mononuclear and polynuclear complexes [6]. However, by far in literature, most of the studies employing this ligand are focused on metals from the lanthanide series. An attempt to pair this ligand with first and second row transition metals for the synthesis of metal complexes is the novel idea being the focus in this study. Hence, in this work we aim to explore the effect of coordinating different

transition metal cations to 3,6-bis-(3,5-dimethylpyrazolyl) pyridazine, follows by investigation and characterization on the electrochemical behavior of the resulting metal complexes.

Materials and Methods

Chemicals and reagents

3,5-dimethylpyrazole ($C_5H_8N_2$, 99%, Aldrich), 3,6-dichloropyridazine ($C_4H_2Cl_2N_2$, 97%, Aldrich), copper(II) chloride dihydrate ($CuCl_2 \cdot 2H_2O$, 99%, Aldrich), iron(II) chloride tetrahydrate ($FeCl_2 \cdot 4H_2O$, 99%, Aldrich), nickel(II) chloride hexahydrate ($NiCl_2 \cdot 6H_2O$, 99%, Aldrich), cobalt(II) nitrate hexahydrate ($Co(NO_3)_2 \cdot 6H_2O$, 98%, Aldrich), sodium hydride (NaH, 90%, Aldrich) and anhydrous dimethylformamide (99.8%, Aldrich) were used as such without further purification.

Synthesis of 3,6-bis(3,5-dimethylpyrazolyl) pyridazine

As shown in Figure 1, 3,5-dimethylpyrazole (240.3 mg, 2.5 mmol) and sodium hydride (103.6 mg, 2.5 mmol) were put in the reaction flask under nitrogen gas purging. Anhydrous dimethylformamide (5 mL) was added into the flask. After one hour stirring, the solution was cooled to 0 °C after being kept in an ice bath. 3,6-dichloropyridazine (148.9 mg, 1.0 mmol) was added to the solution and the temperature was maintained at 0 °C for 30 minutes while stirring. The solution was stirred overnight at ambient temperature to yield the desired ligand. The resulting pale-yellow solution was mixed into ice water (100 mL) to obtain white filtrate solid. Synthesis route of the preparation is shown in Figure 2.

Synthesis of transition metal complexes

DPPMe (53.67 mg, 0.20 mmol) was dissolved in chloroform, CHCl₃ (5 mL). The appropriate metal salt (0.40 mmol) was dissolved in MeOH (5 mL) separately and was added dropwise into the previous solution. A colored solid precipitated immediately. The solution was continuously stirred for five hours. The precipitate was filtered and washed with methanol followed by

drying in oven. Table 1 shows the mass of metal salts used in each complex.

Characterization

The proton nuclear magnetic resonance, ¹H-NMR for the ligand was measured by using the Bruker Advance 400. Deuterated chloroform, CDCl₃ was used as the solvent. Infrared spectra were obtained using attenuated total reflection (ATR) with model Perkin-Elmer 400 FT in the range of 4000-400 cm⁻¹. Carbon, Hydrogen and Nitrogen (CHN) analyzer of model TrueSpec Micro was used to analyze the ligand and metal complexes to determine respective elemental composition. Energy dispersive X-ray spectrometry was performed using INCAEnergy200 to determine the presence and distribution of the transition metal atoms in the metal complexes.

Solubility test

Solubility test was done on each of the synthesized metal complexes. Approximately 5 mg of the complex was measured and put into the test tubes containing various solvents such as chloroform, dimethyl sulfoxide, acetonitrile, ethanol, methanol, dimethyl formamide and tetrahydrofuran. The solubility of the complexes in each of the solvent was observed. The same procedure was repeated for the DPPMe ligand.

Electrochemical study

The electrochemical measurements were performed using potentiostat (AUTOLAB/PGSTAT 302N) which was run by Analysis of Variance software (ANOVA) installed in the computer. Ag/AgCl, platinum rod, and glassy carbon were used in the setup. Prior to the measurement, the metal complex solution was drop-casted on the glassy carbon electrode and left to dry overnight. A thin film of the metal complex was formed on the electrode. All the measurements were performed at room temperature in the potential range from -1.2 V to +1.6 V vs. Ag/AgCl with a scan rate from 10-100 mV s⁻¹ and 0.10 M tetrabutylammonium perchlorate [Bu₄N(ClO₄)] was used as supporting electrolyte in dimethylformamide.

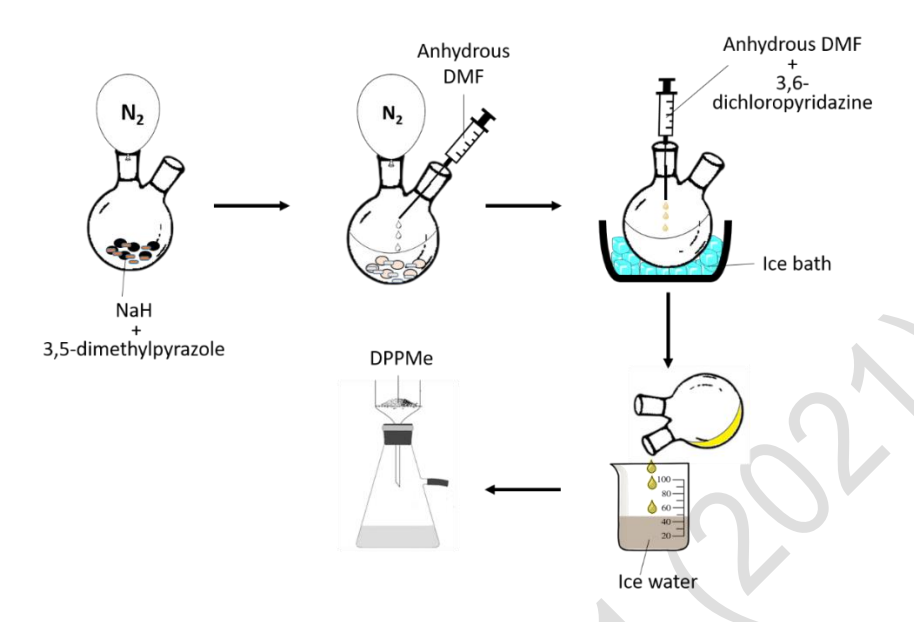


Figure 1. Reaction scheme for synthesis of DPPMe ligand

Figure 2. Synthetic route of DPPMe ligand

Table 1. Mass of metal salts used

Metal Salt	Mass (mg)	Yield Color	Designation
CuCl ₂ ·2H ₂ O	34.10	Pale green	Complex 1
FeCl ₂ ·4H ₂ O	39.76	Dark red	Complex 2
NiCl ₂ ·6H ₂ O	47.54	Dark green	Complex 3
CoNO ₃ ·6H ₂ O	47.59	Dark orange	Complex 4

Results and Discussion ¹H-NMR spectra of DPPMe ligand

The $^{1}\text{H-NMR}$ spectrum of the ligand was analyzed in CDCl₃ from δ 0.00 – 12.00 ppm. From the spectrum (Figure 3), it shows that the 3,6-dichloropyridazine has been successfully reacted to 3,5-dimethylpyrazole. The

singlet peak attributed to the methyl protons is shifted to the upfield at δ 2.22 ppm (H-1) as they were close to the electrons in the ring structure which creates a deshielding effect from its huge anisotropic field. [7]. Furthermore, the protons in the aromatic ring of the pyridazine appeared as doublets and gave two different

signals at δ 7.50 ppm (H-4) and δ 8.11 ppm (H-5). The proton in the pyrazole ring gives rise a singlet peak as there is no neighboring protons to couple with at δ 6.09 ppm (H-3). The assignation of chemical shifts is summarized in Table 2.

IR spectra of DPPMe ligand and the metal complexes

IR spectroscopy confirmed the introduction of the 3,5dimethylpyrazole into the pyridazine molecule at position 3 and 6 was confirmed by the appearance of new peaks in the spectrum. Figure 4 shows the IR spectrum of the ligand with each peak assignment color coordinated to its corresponding functional group. The spectrum exhibited new absorption peak at 2926 cm⁻¹ which is attributed to the methyl group attached to the pyrazole group [8]. The absorption peaks observed at 1443 cm⁻¹ and 1137 cm⁻¹ correspond to the C-N and C=N stretching of the pyrazole structure respectively [9]. Besides that, the stretching of N-N in the pyridazine and pyrazole group has its own characteristic absorption peaks at 970 cm⁻¹ and 1312 cm⁻¹, respectively. The C=N belonging to the pyridazine group was found at 1162 cm⁻¹ [10]. When compared to the spectrum of the ligand as in Figure 5, the band attributed to C=N in the pyrazole ring at around 1125-1129 cm⁻¹ in the metal complexes was shifted to lower wavenumber proving that the metal ion did form a bond with the nitrogen atom in the pyrazole structure [11]. The infrared band obtained at 1162 cm⁻¹ in the free ligand spectrum corresponding to C=N of the pyridazine ring, has been shifted to a higher frequency region at 1168-1171 cm⁻¹ in the metal complexes, indicating the participation of the pyridazine ring nitrogen atom as a possible bonding site. IR band observed at 970 cm⁻¹ of N-N in the pyridazine, was also found shifted to a higher frequency region 988-996 cm⁻¹ in complexes, which provide further information on the presence of pyridazine ring nitrogen atom in bonding. Table 3 summarized the comparison of infrared bands shifting.

Solubility test of synthesized metal complexes

The coordination of metal ions with the ligand had changed the solubility properties of the complexes as presented in Table 4 which proves that the complexation of the metal with the ligand has been successfully

occurred. The solubility studies also help in identifying the suitable solvent used in the electrochemical studies.

Elemental analyses

The complexation of the metal with the ligand resulted in different percentages of carbon, hydrogen and nitrogen of the complexes as tabulated in Table 5. Complex 3 and 4 show a higher deviation in the percentage of the carbon which probably due to the presence of unreacted metal salts in the complex.

UV-Vis spectroscopy spectrum of the metal complexes

Figure 6 displays the UV-Vis spectra for both ligands and its metal complexes 1-4. All the solutions were prepared with the same concentration. From the spectrum, it can be observed that there are three maximum peaks at 246, 259 and 271 nm appearing within the absorption band ranging from 200-300 nm. These three peaks originated from HOMO \rightarrow LUMO π \rightarrow π^* transitions of the pyridazine and pyrazoles groups [12]. The absorption pattern portrayed by the metal complexes are significantly different than the free ligand. All the complexes exhibited a shift in the position of the characteristic ligand band at around 260 nm. This shift is significant as it proves that the metal ion successfully coordinates with the pyridazine and pyrazole rings in the ligand structure.

Energy-Dispersive X-ray spectrum of the metal complexes

EDX analysis (Figure 7) was performed to investigate the elements present in the metal complexes. All the materials used in the synthesis of each metal complexes can be observed which further confirms the complexation of the transition metal to the ligand. The presence of higher percentage of Cl atom in all the metal complexes is due to metal salt used in the reaction and the byproduct formed from 3,6-dichoropyridazine compound after the complexation process. All metal complexes were synthesized using their respective chloride salt.

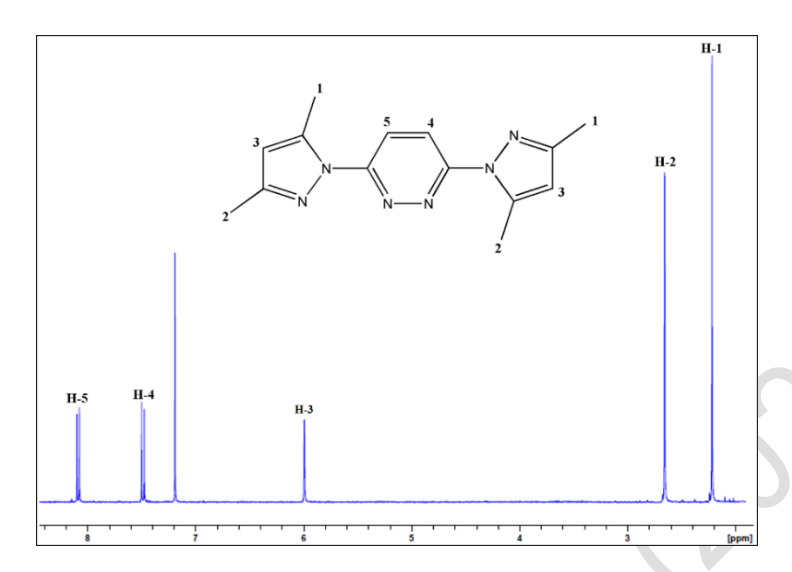
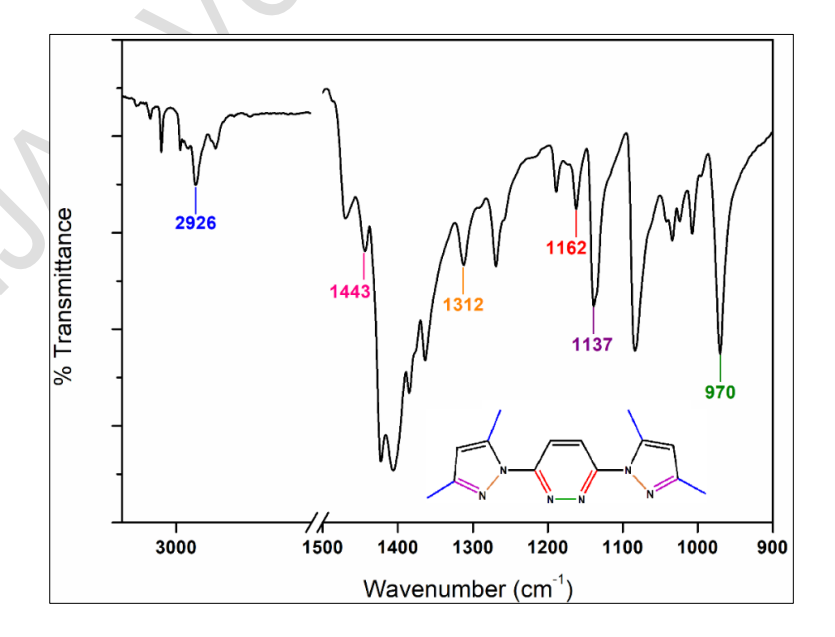


Figure 3. ¹H-NMR spectrum of 3,6-bis(3,5-dimethylpyrazolyl) pyridazine

Table 2. ¹H-NMR chemical shifts assignation

H-position	Integrations	Chemical shift, δ (ppm)	Multiplicity
1	6H	2.22	S
2	6H	2.66	S
3	2H	6.09	S
4	1H	7.50	d
5	1H	8.11	d



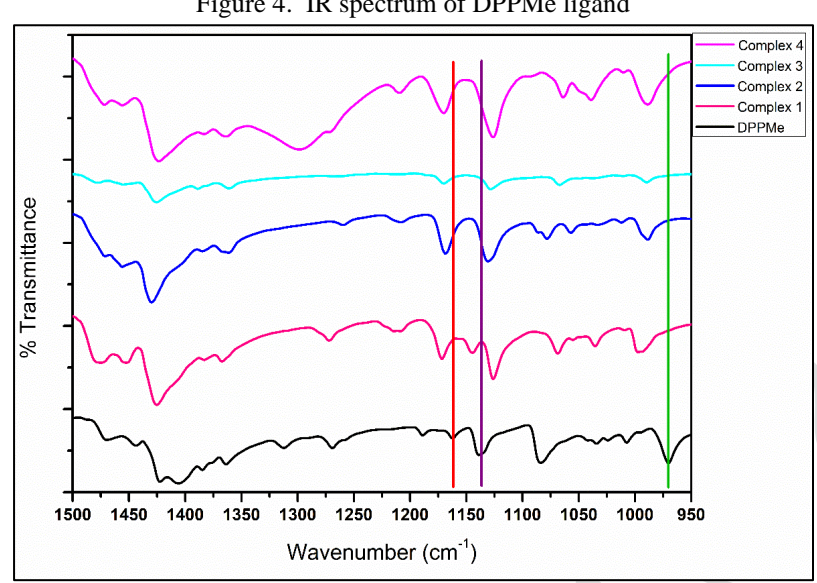


Figure 4. IR spectrum of DPPMe ligand

Figure 5. FTIR spectra comparison of DPPMe ligand and its metal complexes

Table 3. FTIR frequencies (in cm ⁻¹) of DPPMe and its metal co	complexes
--	-----------

Compound	Pyrazole Ring (C=N)	Pyridazine Ring (C=N)	Pyridazine Ring (N-N)	Methyl Group (C-H)	
DPPMe	1137	1162	970	2926	
Complex 1	1125	1171	996	2922	
Complex 2	1129	1168	988	2923	
Complex 3	1127	1169	989	2922	
Complex 4	1126	1170	988	2925	

Table 4. Solubility of DPPMe and its metal complexes

Solvent	Solubility of DPPMe	Solubility of Metal Complexes 1-4
Chloroform	✓	✓
Dimethyl sulfoxide (DMSO)	×	\checkmark
Acetonitrile	×	\checkmark
Ethanol	×	\checkmark
Methanol	×	\checkmark
Dimethyl formamide (DMF)	*	\checkmark
Tetrahydrofuran (THF)	×	✓

Table 5. The percentages of carbon, hydrogen, and nitrogen in the complexes

Compound	Proposed	C%		Н%		N%	
Compound	Empirical Formula	Observed	Calculated	Observed	Calculated	Observed	Calculated
DPPMe	$C_{17}H_{28}N_6$	62.70	64.52	8.58	8.92	32.34	26.56
Complex 1	$[Cu_{2}(C_{17}H_{28}N_{6})\cdot 4Cl$	33.03	34.88	3.12	4.82	14.31	14.36
Complex 2	$[Fe_{2}(C_{17}H_{28}N_{6})\cdot 4Cl$	33.41	35.82	3.87	4.95	14.20	14.75
Complex 3	$[Ni_{2}(C_{17}H_{28}N_{6})\cdot 4Cl$	27.14	35.47	5.87	4.90	14.38	14.60
Complex 4	$[Co_{2}(C_{17}H_{28}N_{6})\cdot 4NO_{3}$	19.95	47.01	5.50	6.50	18.92	19.35

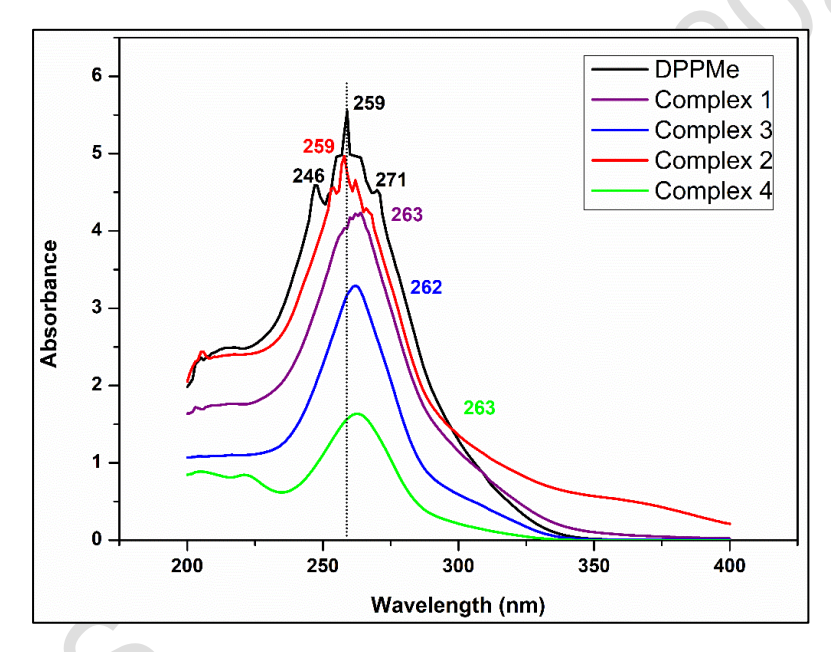
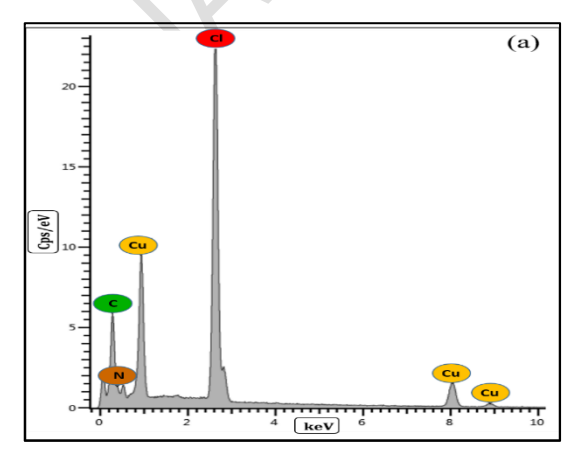
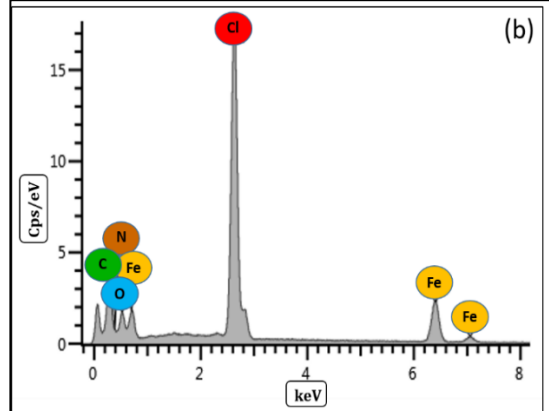
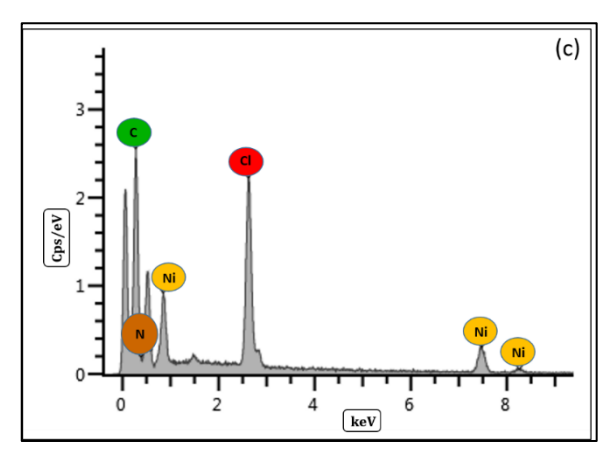


Figure 6. UV-Visible spectra of DPPMe and its metal complexes







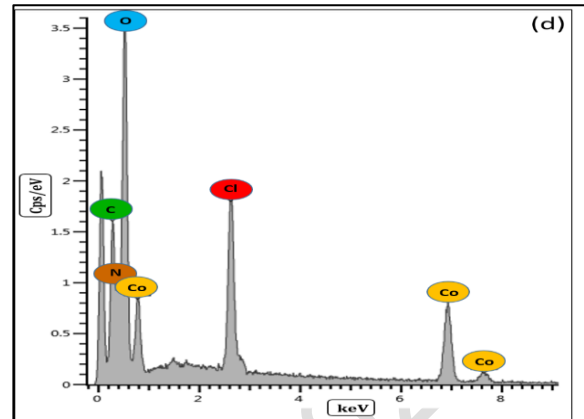


Figure 7. EDX spectrum of the metal complexes (a) Complex 1, (b) Complex 2, (c) Complex 3, (d) Complex 4

Electrochemical studies

From the cyclic voltammogram displayed in Figure 8, complexes 1-3 show a similar pattern which exhibits one electron quasi reversible transfer process with an oxidation peak (Epa) at the forward scan rate and its corresponding reduction peak at the reverse scan rate. The cathodic peak detected in complex 1 at 0.03 V is due to the reduction of Cu(II) to Cu(I). When the scan is reversed, the anodic peak at 0.75 V indicates the oxidation of Cu(I) to Cu(II). Similarly, in complex 2, a cathodic peak is observed at -0.47 V when Fe(II) is oxidized to Fe(III) while its corresponding anodic peak at -0.67 V is formed when Fe(III) is reduced back to Fe(II). Finally, the peak at 0.71 V in complex 3 is attributed to the oxidation of Ni(I) to Ni(II) and the peak at 0.12 V is due to the reduction of Ni(II) to Ni(I). Apart from that, a small reduction peak can be observed at -0.84 V vs. Ag/AgCl at the reverse scan rate for complex 1 while in complex 3 another reduction peak appears at -0.74 V. However, complex 4 did not show any peaks throughout the scan. This could be explained due to the incomplete complexation of cobalt metal and the ligand in complex 4 which can be governed by a few factors such as the metal to ligand ratio, pH and temperature of the synthesis reaction. The alteration in these parameters could lead to a successful complexation in between cobalt and the ligand.

In Figure 9, the cyclic voltammogram of all three complexes in different scan rates were shown in which it can be clearly observed that there was a significant shift in the peak potential during the forward scan towards a more positive potential while in the reverse scan the shift was towards negative value. This behavior is typical for a quasi-reversible system. A significant difference in the quasi reversible voltammogram can be noticed as it displays a large peak-to-peak separation as compared to reversible processes [13]. Theoretically, the process is termed as quasi reversible when the charge transfer and mass transport on the electrode interface does not comply with Nernst equilibrium [14]. There a few properties that shows the cyclic voltammogram is a quasi-reversible such as when the I_p increases with scan rate, it is not proportional to it and the E_{pc} shifts negatively with increasing v. The peak potentials and peak separation of the metal complexes has been tabulated in Table 6.

The electron transfer process which happened on the electrode for each metal complexes was determined by plotting the peak currents (I_{pa} and I_{pc}) against the scan rates and the square root of the scan rates, respectively. In order to calculate the electrochemical transfer kinetic parameters of the metal complexes, Laviron's Equations (1 and 2) were used.

$$E_{pa} = a + \frac{2.303 \, RT}{(1 - \alpha)nF} \log \upsilon \tag{1}$$

$$E_{pc} = b + \frac{2.303 \, RT}{\alpha nF} \log v \tag{2}$$

This parameter includes the number of electrons transfer (η) and the electron transfer coefficient (α) [15]. Based on the graph plotted, Figure 10 indicates the complexes 1-3 exhibit a mass diffusion-controlled process as the anodic and cathodic peak current increase linearly to the square root of the scan rate (\sqrt{v}) [16].

The redox peak potentials and scan rates from 20-100 mVs⁻¹ in logarithmic scale was plotted in Figure 11. It was found to be linear to each other as depicted in

Figure 11. The slopes derived from plot were applied in equation 1 and 2 to extract information on the number of electrons (η) and electron transfer coefficient (α). For complex 1, the number of electrons is estimated to be $0.74 \approx 1$ and the α is 0.38. Hence, the electrochemical redox process of complex 1 ($Cu^{2+} \rightleftharpoons Cu^{+}$) required one electron. The slope of complex 2 shows the number of electrons to be $0.55 \approx 1$ and the α is 0.36. Complex 2 also shows a one electron transfer electrochemical redox process ($Fe^{2+} \rightleftharpoons Fe^{3+}$). Finally, for complex 3, the number of electrons is estimated to be $0.66 \approx 1$ and the α is 0.54. Thus, it also shows a one electron transfers redox process ($Ni^{2+} \rightleftharpoons Ni^{+}$).

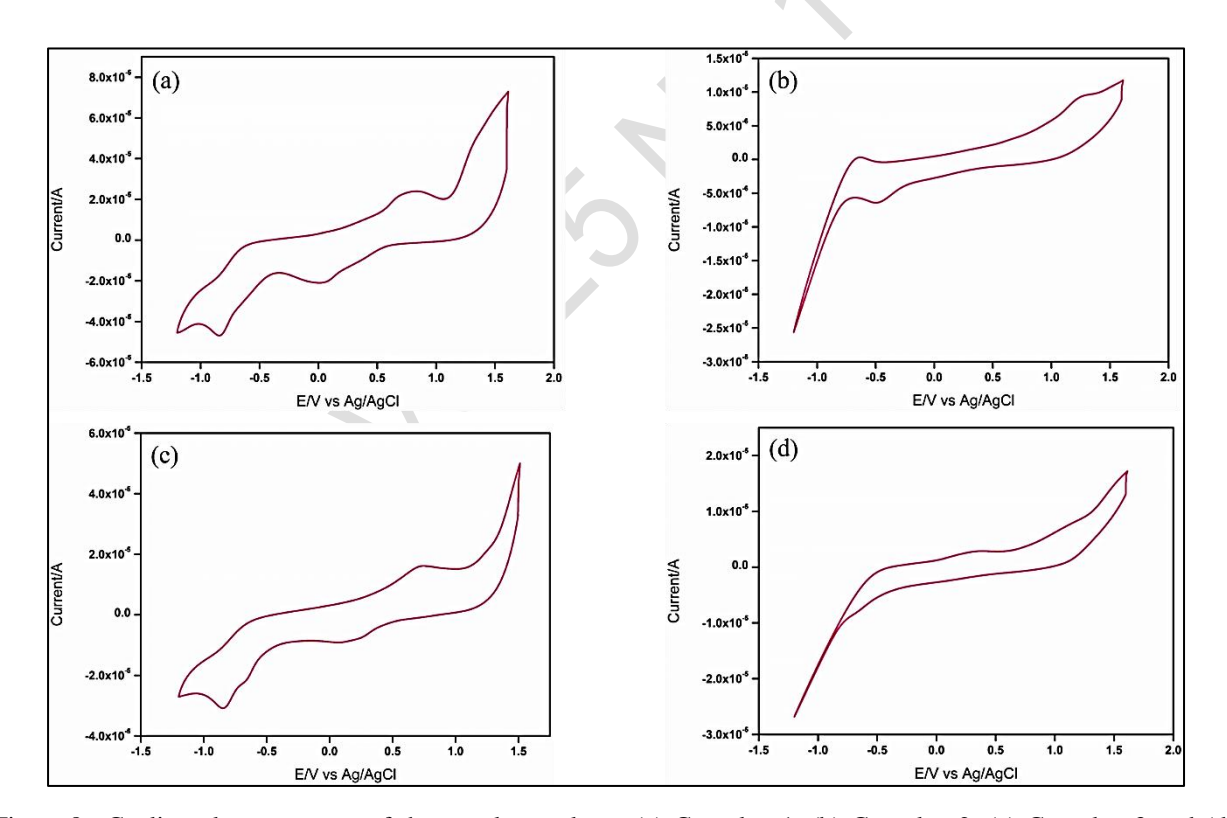


Figure 8. Cyclic voltammograms of the metal complexes (a) Complex 1, (b) Complex 2, (c) Complex 3 and (d) Complex 4 at a scan rate of 100 mV s⁻¹ in the presence of 100 mM tetrabutylammonium perchlorate, [Bu4N(ClO4)] in DMF electrolyte solution. Scanning was performed against Ag/AgCl (sat. KCl) reference electrode

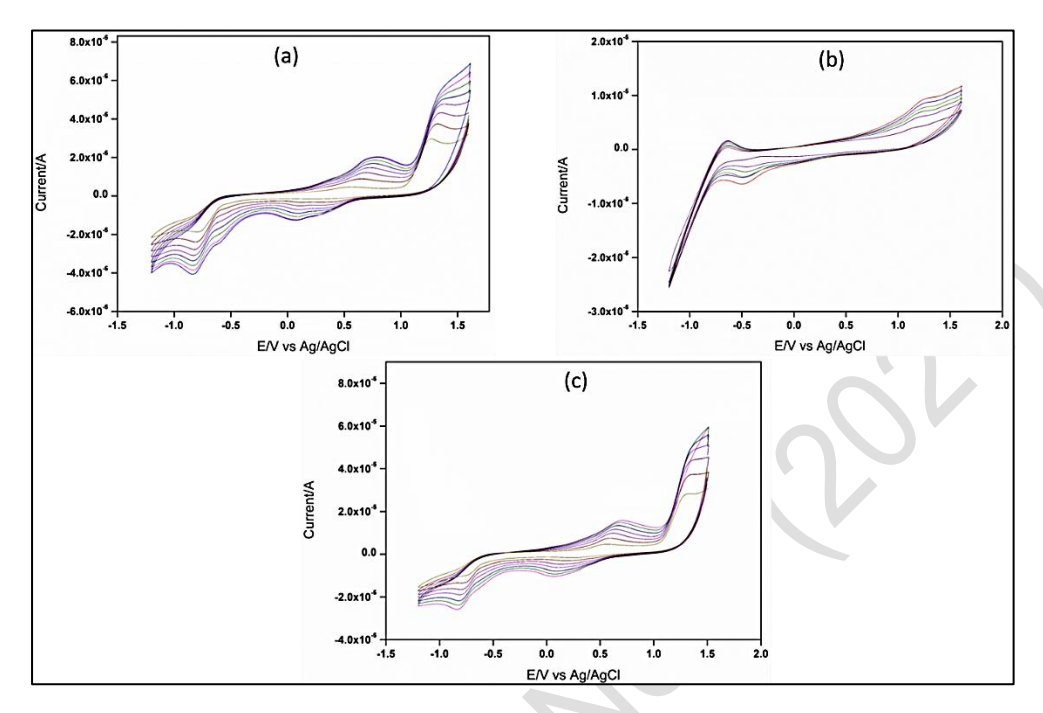


Figure 9. Cyclic voltammograms of the metal complexes (a) Complex 1, (b) Complex 2 and (c) Complex 3 at a scan rates of $20\text{-}90 \text{ mVs}^{-1}$

Table 6. Peak potentials and peak separation of complex 1-3

Compound	E _{pa} (V vs Ag/AgCl)	E _{pc} (V vs Ag/AgCl)	ΔE (V vs Ag/AgCl)
Complex 1	0.75	0.03	0.72
Complex 2	-0.67	-0.47	0.20
Complex 3	0.71	0.12	0.59

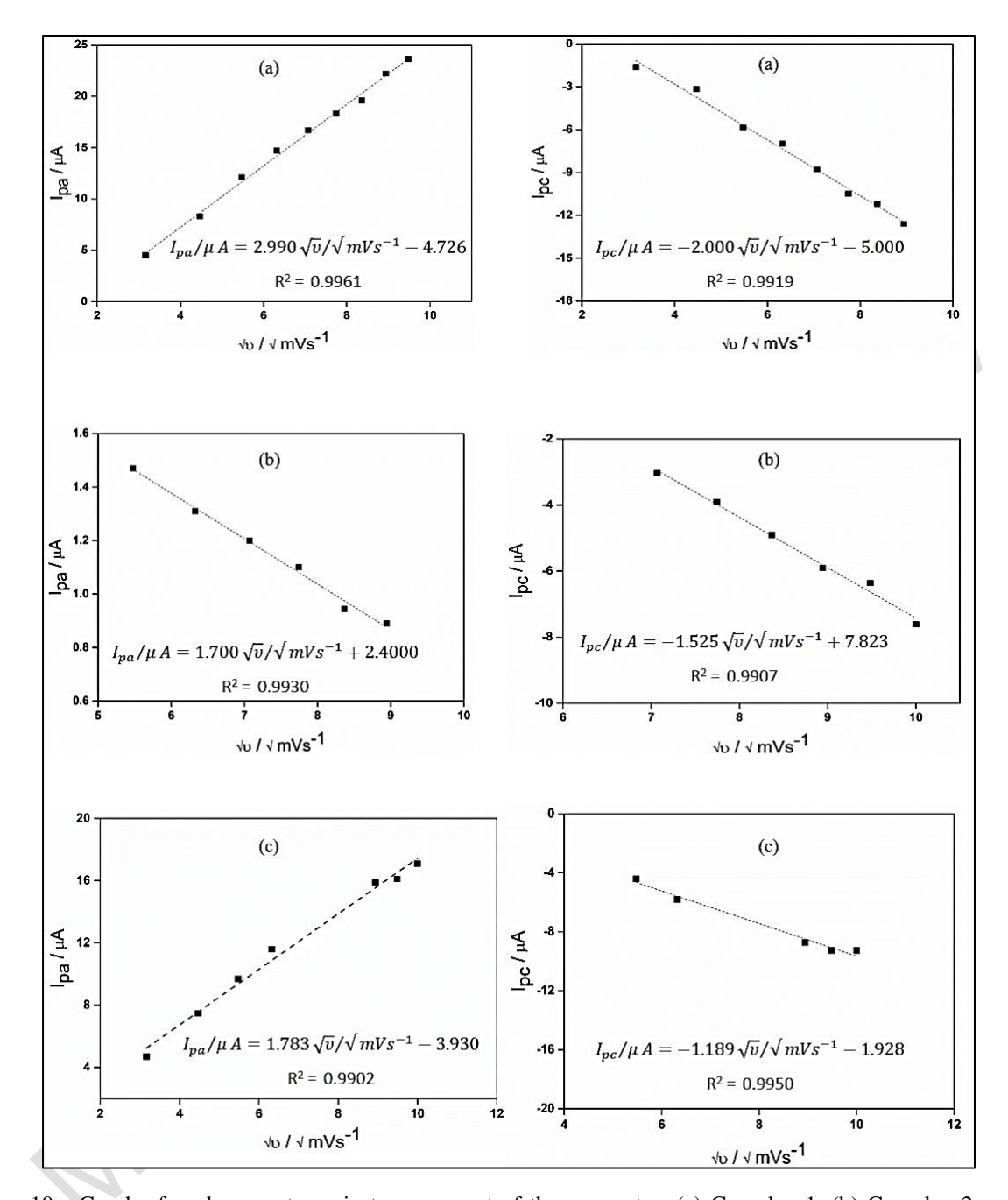


Figure 10. Graph of peak currents against square root of the scan rates: (a) Complex 1, (b) Complex 2 and (3) Complex 3

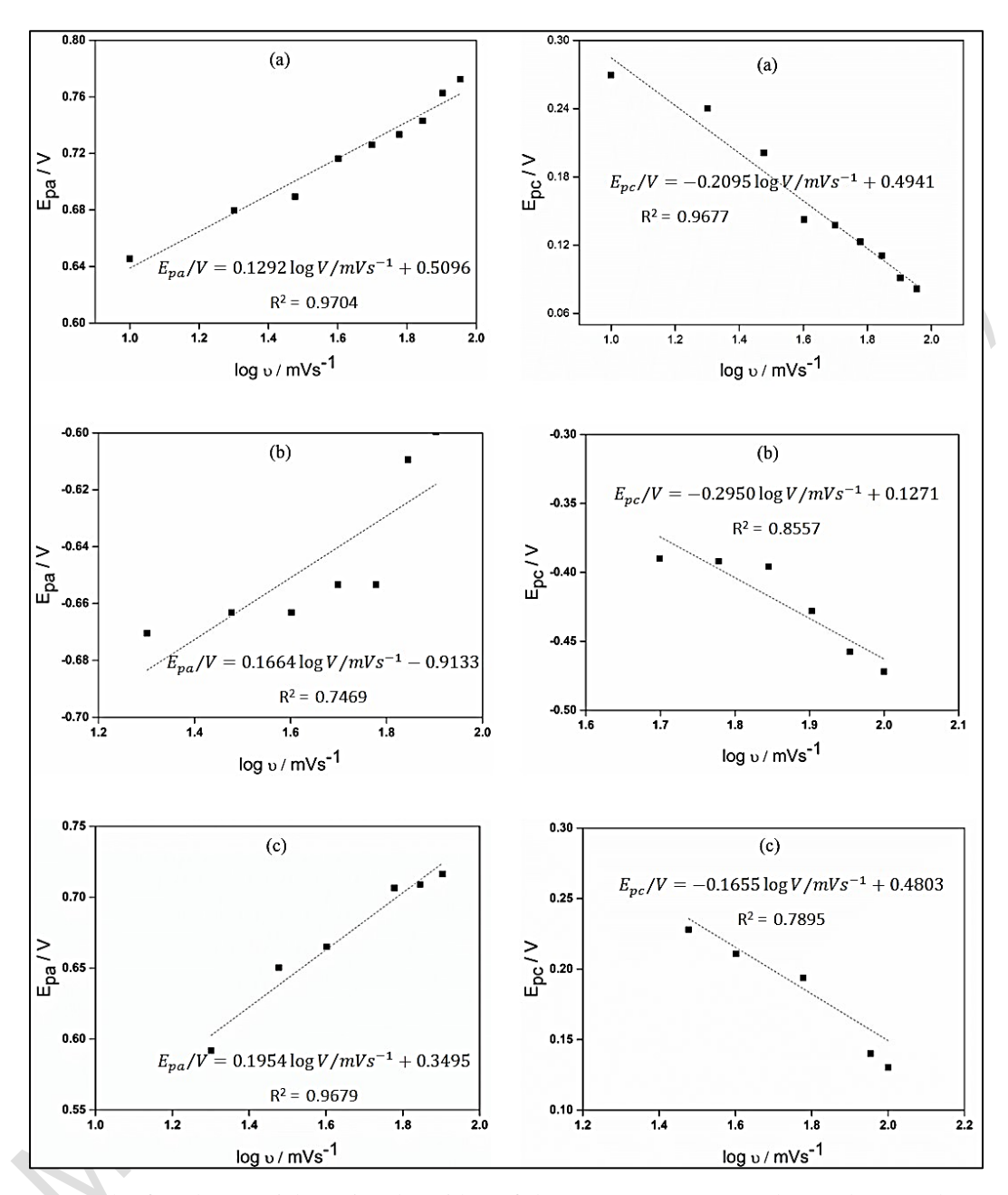


Figure 11. Graph of peak potentials against logarithm of the scan rates: (a) Complex 1, (b) Complex 2 and (3) Complex 3

Conclusion

In this project, 3,6-bis (3,5-dimethylpyrazol-1yl) pyridazine ligand has been successfully synthesized through several steps of reactions. The structure produced through the reaction of 3,5-dimethylpyrazole

with 3,6-dichloropyridazine was confirmed by using IR and ¹H NMR spectral analyses. The ligand was then complexed with Cu(II), Fe(II), Ni(II) and Co(II) transition metals to form four novel coordinated complexes named as complex 1, complex 2, complex 3

and complex 4 respectively. Subsequently, the complexation of the metals to the ligand was affirmed through several analyses. The IR spectra of the metal complexes displayed significant shifts in several peaks of the functional groups present in the ligand. Furthermore, the UV-Vis analysis confirmed the complexation when the spectrum showed a prominent shift at ligand band characteristic at around 260 nm. The stoichiometry of the complexes was determined based on the elemental analyses and the empirical formula for each complex were proposed as [Cu₂(C₁₇H₂₈N₆).4Cl], $[Fe_2(C_{17}H_{28}N_6).4Cl],$ $[Ni_2(C_{17}H_{28}N_6).4Cl]$ [Co₂(C₁₇H₂₈N₆).4NO₃], respectively. EDX analysis was used to confirm the presence of the metals in the complexes. Finally, cyclic voltammetry analysis was performed on all the complexes to study its electrochemical properties. Complex 1, 2 and 3 showed quasi-reversible of one electron transfer process with oxidation peaks at 0.75 V, -0.67 V and 0.71 V respectively whereas its corresponding reduction peaks at 0.03 V, -0.47 V and 0.12 V. Complex 4 did not show any peaks throughout the forward and reversed scans. In future, the effect of the complex solubility in different organic solvents on its electrochemical behavior will be studied. The complexes will also be explored in electrochemical applications such as electrocatalytic dye degradation and electrocatalyst for water splitting process.

Acknowledgement

This research is supported by the Interdisciplinary Research Program Grant (IIRG013B-2019) given by the Universiti Malaya. The work was also supported by the IMRC/AISTDF/CRD/2018/000048 (ASEAN-India Collaborative R&D Scheme).

References

- Cargnelutti, R., Schumacher, R. F., Belladona, A. L. and Kazmierczak, J. C. (2021). Coordination chemistry and synthetic approaches of pyridylselenium ligands: A decade update. *Coordination Chemistry Reviews*, 426: 213537.
- Dubois, D. L. (1997). Development of transition metal phosphine complexes as electrocatalysts for CO₂ and CO reduction. *Comments on Inorganic Chemistry*, 19(5): 307-325.

- Cheung, K.-C., Wong, W. L., Ma, D. L., Lai, T. S. and Wong, K. Y. (2007). Transition metal complexes as electrocatalysts-Development and applications in electro-oxidation reactions. *Coordination Chemistry Reviews*, 251(17): 2367-2385.
- 4. Grünwald, K. R., Saischek, G., Volpe, M., Belaj, F. and Mösch-Zanetti, N. C. (2010). Pyridazine-Based ligands and their coordinating ability towards first-row transition metals. *European Journal of Inorganic Chemistry*, (15): 2297-2305.
- 5. Viciano-Chumillas, M., et al. (2010). Coordination Versatility of Pyrazole-Based Ligands towards High-Nuclearity Transition-Metal and Rare-Earth Clusters. *European Journal of Inorganic Chemistry*, (22): p. 3403-3418.
- 6. Gao, H., Tanase, S., de Jongh, L. J. and Reedijk, J. (2006). Synthesis, crystal structures and properties of the novel mononuclear copper(II) and tetranuclear cobalt(II) complexes with 3,6-bis-(3,5-dimethylpyrazolyl)-pyridazine. *Transition Metal Chemistry*, 31(8): 1088-1092.
- 7. Baranac-Stojanović, M. (2014). New insight into the anisotropic effects in solution-state NMR spectroscopy. *RSC Advances*, 4(1): 308-321.
- 8. Kaddouri, Y., Abrigach, F., Mechbal, N., Karzazi, Y., El Kodadi, M., Aouniti, A. and Touzani, R. (2019). Pyrazole compounds: Synthesis, molecular structure, chemical reactivity, experimental and theoretical DFT FTIR spectra. *Materials Today: Proceedings*, 13: 956-963.
- 9. Anush, S. M., Vishalakshi, B., Kalluraya, B. and Manju, N. (2018). Synthesis of pyrazole-based Schiff bases of Chitosan: Evaluation of antimicrobial activity. *International Journal of Biological Macromolecules*, 119: 446-452.
- Figueiredo, H., Silva, B., Raposo, M. M. M., Fonseca, A. M., Neves, I. C., Quintelas, C. and Tavares, T. (2008). Immobilization of Fe(III) complexes of pyridazine derivatives prepared from biosorbents supported on zeolites. *Microporous and Mesoporous Materials*, 109(1): 163-171.

- Mészáros Szécsényi, K., Leovac, V. M., Jacimovic, Z. K. and Pokol, G. (2003). Transition Metal Complexes with Pyrazole Based Ligands. *Journal* of Thermal Analysis and Calorimetry, 74(3): 943-952.
- 12. Mezei, G. and Raptis, R. G. (2004). Effect of pyrazole-substitution on the structure and nuclearity of Cu(II)-pyrazolato complexes. *Inorganica Chimica Acta*, 357(11): 3279-3288.
- 13. Kutluay, A. and Aslanoglu, M. (2013). Modification of electrodes using conductive porous layers to confer selectivity for the voltammetric detection of paracetamol in the presence of ascorbic acid, dopamine and uric acid. *Sensors and Actuators B: Chemical*, 185: 398-404.
- Beaver, B. D., Hall, L. C., Lukehart, C. M. and Preston, L. D. (1981). Reactions of coordinated molecules. XXVII. Cyclic voltammetry of several transition metal metalla-acetylacetonate complexes. *Inorganica Chimica Acta*, 47: 25-30.
- 15. Huang, F., Wang, F., Feng, S., Li, Y., Li, S. and Li, Y. (2013). Direct electrochemistry and electrochemical biosensing of glucose oxidase based on CdSe@CdS quantum dots and MWNT-modified electrode. *Journal of Solid State Electrochemistry*, 17(5): 1295-1301.
- 16. Hamel, C., Chamelot, P. and Taxil, P. (2004). Neodymium(III) cathodic processes in molten fluorides. *Electrochimica Acta*, 49(25): 4467-4476.